Modeling the Plastic Strain of 48" UF_6 Cylinders Exposed to the IAEA Fire Test

G.H. Bailey, G.W. Monks
BNFL International Group

INTRODUCTION

As part of the continuing review of its regulations for the transport of radioactive materials, the IAEA has established a Coordinated Research Programme to study the behaviour of UF_6 cylinders under fire exposure conditions. This Paper provides a review of recent work by British Nuclear Fuels plc, associated with that CRP.

Earlier modelling studies have shown that the bounds of uncertainty on the available models meant that neither survival nor failure of a fully loaded 48" UF_6 cylinder, exposed to the standard IAEA fire test, could be confidently predicted.

Plastic strain analysis, taking account of thermal and pressure stresses, has been carried out for the UF_6 cylinder. This finite element computation included heat transfer, thermal stress, and mechanical stress analyses to predict the temperatures, stresses, displacements and strains that could be induced into the structure of the container after 30 minutes exposure to an 800°C fire.

MODEL BASIS

The container was considered in a horizontal position assuming a vapour filled space above the liquid/solid UF_6. The BNFL lumped parameter model Burst3 was used to evaluate the bulk temperatures of the ullage volume and of the liquid UF_6, together with the quantities of the different phases present at the 30 minute point. The finite element analysis program ANSYS was then used for all the vessel structure analysis work.

Only one quarter of the container was modelled because of the symmetry present in the analysis. The model, shown in Figure 1, consisted of approximately 6000, 8-noded

solid elements, which were used to model the conduction heat transfer in the container walls, and their mechanical behaviour. Corresponding surface elements were used to model the radiation and convection boundary conditions.

The temperature and heat transfer conditions used as the input to the thermo-mechanical modelling are summarised on Figure 2. Values for internal emissivities are uncertain, but a figure of 0.6 is judged to be conservative (i.e. a low value leading to high estimates of steel temperature) for the purpose of this analysis. It should be noted that the UF_6 vapour pressure is not necessarily limited to the bulk liquid vapour pressure, since if liquid stratification occurs the interface temperature may be higher.

The key steel properties used are noted on Table 1, using information from Lunt 1991 and from some tests commissioned specifically for this project. From this latter work, we have also measured (but not yet incorporated into the finite element model) the degree of uniform thinning which occured on the tensile test specimens, in order to get a more realistic assessment of the hardening modulus than is obtained from the conventional assessment based on original specimen diameter.

TEMPERATURE PROFILE

Finite element thermal analysis using ANSYS generated the temperature profile illustrated by Figure 3. Obviously those parts of the cylinder in contact with liquid hex are much cooler than other regions. A large temperature gradient occurs in the shell in the region of the liquid/vapour interface. The uppermost areas of the shell reach temperatures of about 660°C, while the areas below liquid level are generally below 300°C. (Internal radiation is significant; initial calculations which did not take it fully into account led to shell temperatures in excess of 700°C, and much reduced burst pressure estimates).

PLASTIC STRAIN EFFECTS

The above temperature profile was taken as input to the strain modelling. The effects are evaluated in terms of Von Mises equivalent plastic strain.

First the plastic strains due to the temperature effects alone were evaluated. Differential thermal expansions resulted in a maximum figure of 1.6%, occurring on the outer edge of the central stiffening ring. Plastic strains of up to about 0.5% occurred in the shell itself, in the areas just above the liquid.

Next the internal surface of the shell was subjected to a gradually increasing pressure, to observe the effects on the strain patterns. Little change in the overall pattern occurred up to a pressure value of 20bar. Most of the cylindrical areas of the shell in contact with hex vapour now show plastic strains of 0.1% to 0.5%.

Increasing the pressure to 30bar further strains the vessel shell. A maximum of 1.6% equivalent plastic strain is now observed, between the stiffening rings and roughly halfway between the vapour/liquid interface and the top of the cylinder. Clearly at this point both differential thermal expansion and pressure are contributing significantly to the stress.

The pressure was further increased to the limit of stable computation. This was at 31.5bar. The resulting plastic strain profile is shown by Figure 4. The point of maximum strain has moved to the top of the shell. There is a maximum of 7.7%, where the topmost part of the shell, between the outer and centre stiffening rings, is starting to 'balloon'. Based on the conventional estimation of hardening modulus, this condition represents the point of instability of the shell, ie further pressure increase will cause a burst.

The absence of significant plastic strain in the region between the outer stiffening ring and the ellipsoidal end/skirt is believed due to two factors.-
(i) The ellipsoidal end provides a much stronger constraint to expansion than do the stiffening rings, and
(ii) The distance between the stiffening rings is much greater than the distance from stiffening ring to ellipsoidal end.

The directionality of the strains, at the area of maximum strain, is as follows:-

- hoop strain + 4.8%
- longitudinal strain - 0.7%
- thickness strain - 4.1%

Clearly hoop stress is the most important, and the figures indicate that failure would be in the form of a tear along the top of the shell. Also, since the highest strain region is relatively small in longitudinal extent, it is reasonable to expect that the length of the tear would be less than the distance between the stiffening rings.

REFINED HARDENING MODULUS

The fact that hoop stress effects predominate, and the failure location has been identified, suggests a means of qualitatively analysing the effects of variations in input data. This is to consider the cylinder as an infinitely long plain shell, ALL held at the same temperature as that determined for the top of the actual shell midway between the stiffening rings. Naturally, such a tube will fail at a lower pressure due to the absence of reinforcement by stiffening rings and dished ends, but the relative effects of variations in input data should provide approximate guidance.

The data given by Table 1 includes hardening modulus estimated on the basis of original test piece diameter (ie using Engineering Stress). Using a True Stress value based on the decreasing test piece diameter as it is stretched results in a more realistic (less conservative) estimate of the strength of the steel as it is stretching up to the point of maximum load. Measurements on the test pieces from the limited BNFL trials indicate that in excess of 10% extension occurs uniformly, up to the point of maximum total force, before 'necking' occurs and total force falls off rapidly. This refinement has not yet been incorporated into the full model, but the principal effects have been considered using the 'infinite length plain shell' model introduced above.

Figure 5 shows the results of this calculation, giving internal pressure as a function of the change in radius. The key difference is that conventional estimates show pressure falling (which equates to failure) after the elastic limit, whereas the refined estimates show pressure continuing to rise after that point.

At a temperature of 660°C which applies in the critical area of the shell as modelled here, it would appear that use of True Stress would increase the pressure required for failure by up to 20%.

CONCLUSIONS

In temperature conditions likely to arise in the IAEA fire test, it appears that internal overpressures in excess of 30bar would be required to cause rupture of a 48" UF_6 cylinder. Whether such pressure will occur is dependent on the detailed thermohydraulic behaviour of the UF_6 itself.

REFERENCES

Lunt, H. E. ASTM Committee A-1 on Steel, Stainless Steel and Related Alloys. 1991 Communication of Interim Data from the Nuclear Systems Materials Handbook.

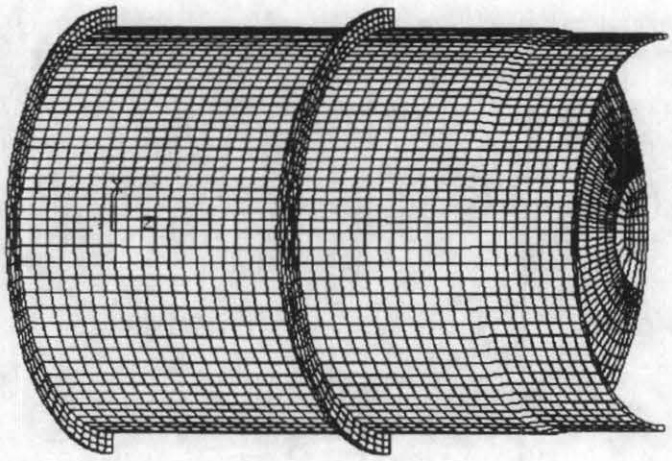

Figure 1. The Finite Element Model

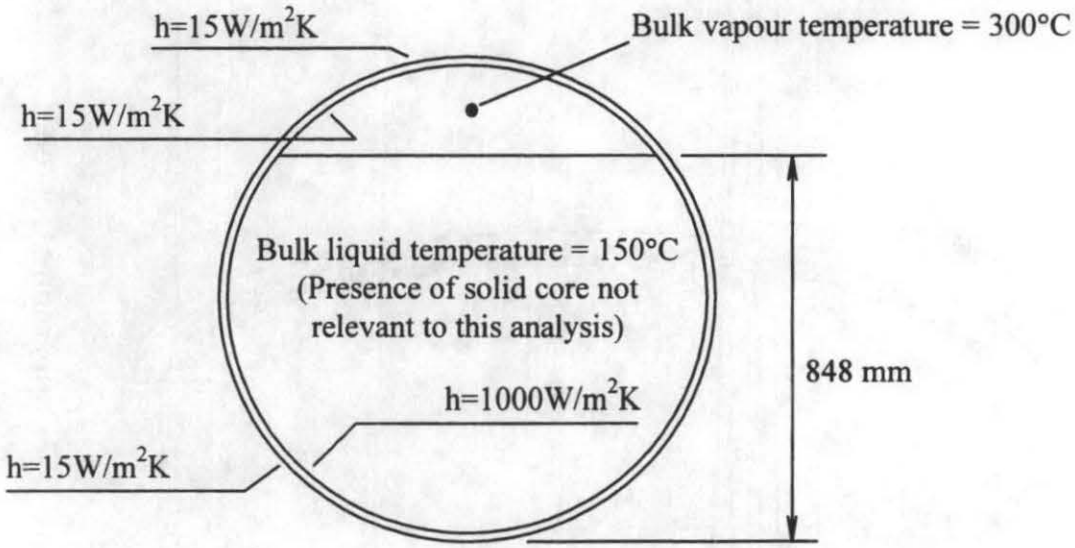

CONVECTION:
Assigned values for the heat transfer coefficient (h) for each region are as shown.

RADIATION:
Emissivity of entire outside of cylinder = 0.8
In the vapour region, emissivity of both steel and hex taken as 0.6
Radiation ignored for the inner surface in contact with liquid.

Figure 2. Thermal Basis

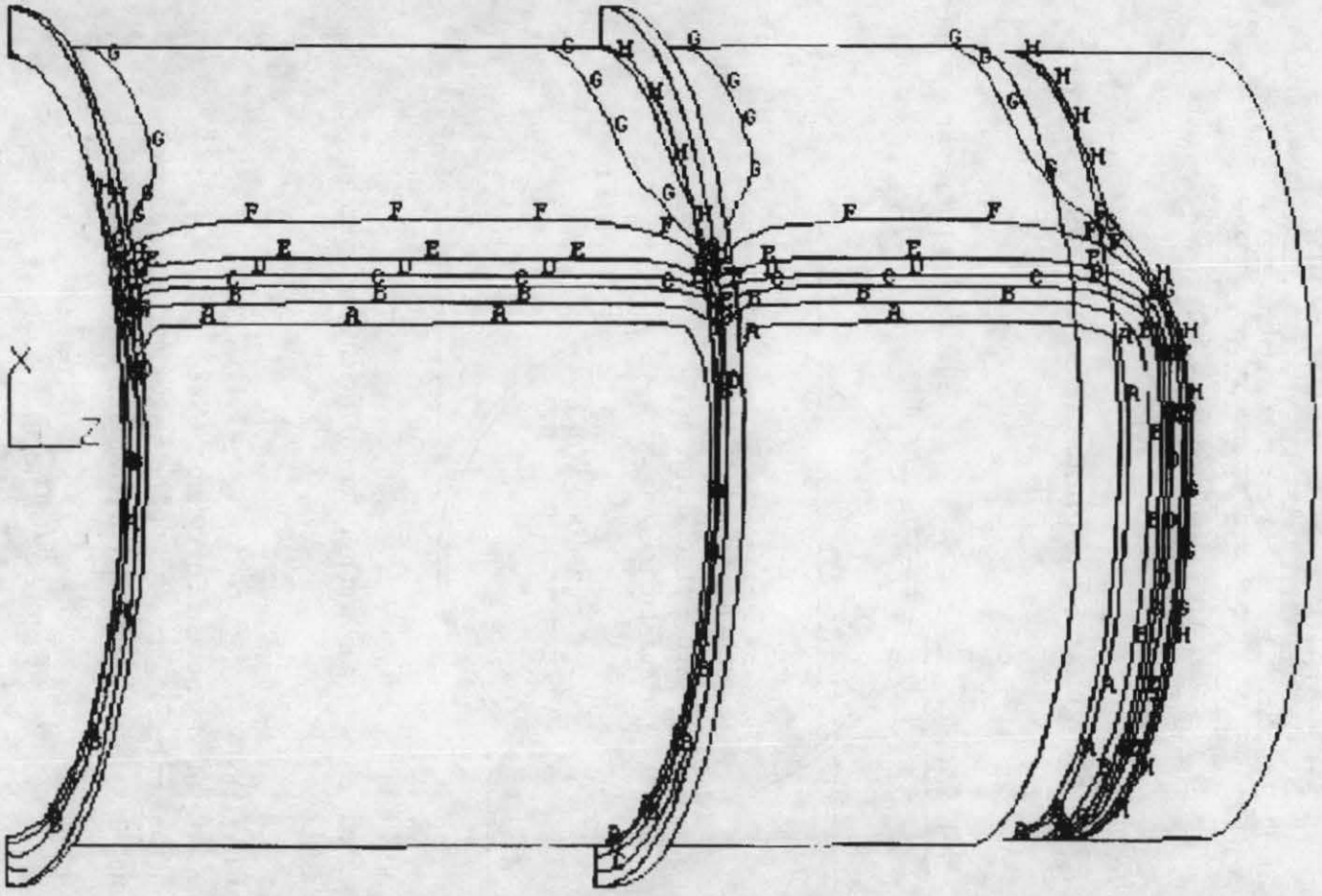

Figure 3. Temperature Contours

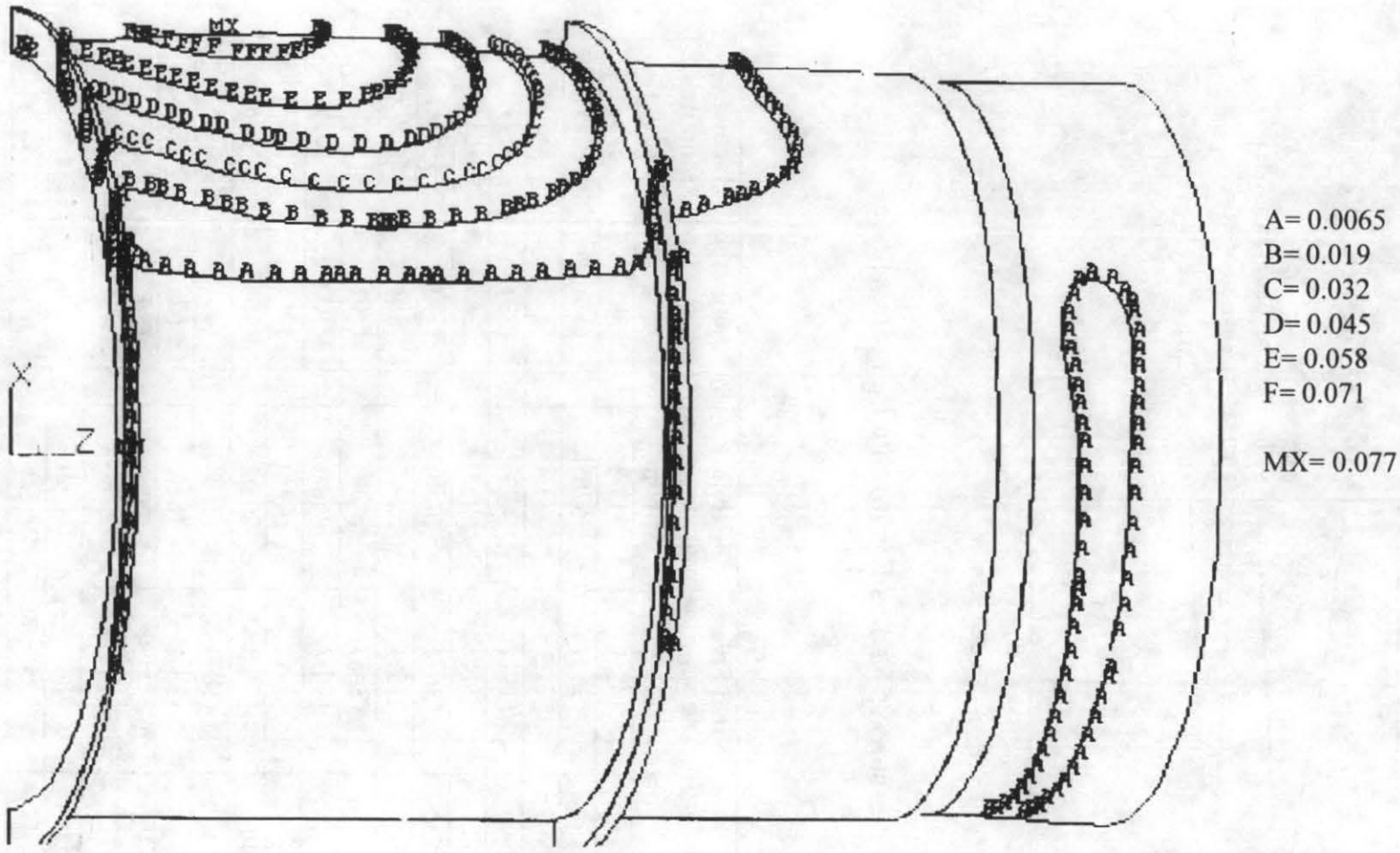

Figure 4. Plastic Strain Contours at 31.5 Bar

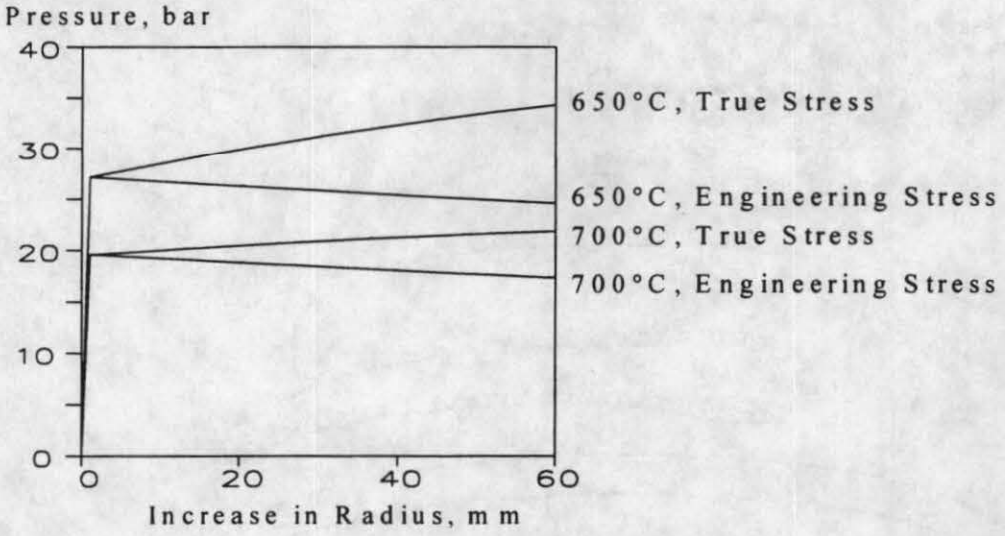

Figure 5. Pressure vs Radius For Infinite Length Cylinder

Temperature °C	Yield Stress M N/m^2	Ultimate Tensile Stress M N/m^2	% Elongation	Hardening Modulus M N/m^2
24	302.3	449.8	39	378.2
(24)	(363)	(526)	(31)	(525)
100	277.3	473.4	37	530
(101)	(313)	(472)	(29)	(543)
200	244	502.9	34	761.5
(202)	(267)	(450)	(27)	(691)
300	211.4	529.3	30	1059.6
(303)	(228)	(484)	(30)	(859)
400	194.7	452.1	30	858
(404)	(235)	(447)	(34)	(624)
500	176.8	295.2	40	296
(505)	(187)	(353)	(44)	(375)
600	135.4	181.1	62	73.7
(606)	(132)	(224)	(54)	(170)
700	76.3	92.4	105	15.3
(707)	(80)	(102)	(72)	(30.6)
800	35	52.2	75	22.9

Table 1:

Material Properties For Steel SA-516 Grade 55

The figures in brackets are single test values measured by BNFL.